

Volume 4 Issue X, October 2025, No. 78, pp. 987-1002 Submitted 2/9/2025; Final peer review 10/10/2025 Online Publication 12/10/2025 Available Online at http://www.ijortacs.com

A HYBRID DEEP LEARNING MODEL TO AUTOMATE THE CLASSIFICATION AND SEGMENTATION OF GLIOMA TUMORS FROM MRI MEDICAL IMAGES

^{1*}Oliokwe, Bibian N., ²Chukwu, Chikaodili C.

^{1&2}Computer Science Department Enugu State Polytechnic, Iwollo. Email and Phone: ^{1*}oliokwe.bibian@espoly.edu.ng; 07037457356, ²chukwu.chikaodili@espoly.edu.ng; 08166930726, ^{*}Corresponding Author Email: bibianemehelu@gmail.com

Abstract

Gliomas are among the most aggressive brain tumors experienced and the accurate classification of such disease is critical for effective diagnosis and treatment in patients. Therefore, this study proposes a hybrid deep learning model integrating Convolutional Neural Networks (CNNs), ResNet50, and U-Net to automate the classification and segmentation of glioma tumors from Medical Resonance Imaging (MRI) scans. The proposed model applies CNN for feature extraction in the pipeline, ResNet50 for deep residual learning and U-Net for precise pixel-level tumor localization and a dataset of 10,694 MRI images from 184 subjects, including both primary hospital data and secondary sources from the Roboflow repository, was used for training and validation. The dataset covered four glioma types: Glioblastoma Multiforme (GBM), Meningioma, Ependymomas, and Mixed Glioma. The model was trained using the Adam optimizer with categorical cross-entropy loss over 50 epochs, applying data augmentation to enhance robustness. Experimental results demonstrate that the hybrid model achieved a training accuracy of 95% and validation accuracy of 94%, outperforming standalone CNN and ResNet50 models. Confusion matrix analysis confirmed reliable multi-class classification, while practical testing validated accurate tumor segmentation and labelling. These results indicate that the proposed model provides a robust, scalable, and clinically applicable tool for automated glioma detection, supporting radiologists in diagnostic decision-making.

Keywords: Glioma Classification; MRI; Deep Learning; Convolutional Neural Network (CNN); Brain Tumor Segmentation

1. INTRODUCTION

All over the world, brain tumor has remained a major health concern and has been identified as one of the most terrifying health challenge in the 21st century (Muhammad et al., 2022). These brain tumors are abnormality in the brain cell due to colony of diseases and have remained the main contributor to brain cancer among adults and children. According to Perkins and Liu (2016) brain tumor is classified into two stages which are the primary stages and the secondary stages. The primary brain tumors contributes over 70% of all brain tumor cases, and are of various types which are the malignant, glioma, meningioma and pituitary. These primary brain tumors are normally very small in size during origination and known as benign in medical terms, while the later stage of the tumor is the secondary which is when it has spread to other parts of the body (Sharif et al., 2020). While all these types of the primary brain tumor are deadly, Louis et al.

(2016) submitted that 80% of them are the glioma, thus making it the center of attention for this research. Gliomas are types of brain tumor which originates from the glial cell located at the central nervous system; and are classified into astrocytomas, GlioblastomaMultiforme (GBM), oligodendroglioma, ependymomas, mixed glioma, diffuse intrinsic pontineglioma, andpilocyticstrocytoma (Alqudah et al., 2019). Among which the first three are the most life threatening with particularly GBM the deadliest and survival period of 12-15month even with intensive care and aggressive treatment, therefore timely and accurate classification of brain tumor is vital to enhance chances of survival through immediate treatment and planning.

In many parts of the world today, diagnosing brain tumor is one of the most expensive health care services, even with countries having the most advanced technologies. Coupled with the invasive procedures and time taken to diagnose the patients (Qureshi et al. 2022), the need for a more flexible and easy diagnostic system remained a research attention.

The evolution of Artificial Intelligence (A.I) over the years has continued to improved quality of health care services and has been applied in studied such as (Saman and Narayanan, 2018; Ankita, 2020; Hossain, 2021; Deborah et al., 2022) to solve medical challenges. In the context of brain tumor, Saman and Narayanan (2018) applied image processing techniques for brain tumor segmentation using Magnetic Resonance Imaging (MRI) as data, while the study was able to segment deformed part of the brain to detect tumor, an improved approach using deep learning was presented in Hossain (2021), Algudah et al. (2019) and Ankita (2020), who trained Convolutional Neural Network (CNN) for brain tumor classification. Most recently, Mahmud etal. (2023) trained and compared ResNet, Inception V3, VGG-16, (CNN) with brain tumor data and identified CNN as the best. While these studies have all contributed positively to the classification of brain tumor injuries, solution have not been obtained on research specifically tailored towards the classification of the various glioma brain tumor injuries and this has remained a research lacuna. Therefore, this study proposed a multi-classification system for the early detection of brain tumor using artificial intelligence technique. The study will focus on generating a model which can classify various types of gloimas using A.I. The types of glioma to be considered are astrocytomas, glioblastoma multiforme, oligodendroglioma, which are the main threat types of Glioma.

2. METHODOLOGY

In computer science and software engineering, methodology is of three types which are the research methodology, software development lifecycle and software design methodology. The research methodology used in this case is the experimental method. The software development lifecycle used is the Agile approach while the software design approach used is also the Agile model. The reason for the adoption of this methodology is due to its ability to align with system design scalability (i.e it allows the existing system to modify to fit in new requirements). More so, it allows the system development team to improve quality of the software design and ensure a consistent quality model that guarantees application and user requirements satisfactions.

2.1 Data Collection

The data used for this work was collected from Memfy's Hospital, radiological department, considering glioma infected patients from the age of 25 to 65years. The data collection instrument is the 3T-MRI machines. The particular gliomas considered are meningioma, mixed glioma, ependymomas, and Glioblastoma Multiforme (GBM). The data collection was carried out across different period of the glioma development in the patients over one year. Figure 1 presents the data sample of GBM over one years, with (a) the data collected at the very early state of the GBM which is the first one month, (b) represent data collected after 3 months from the same patients, (c) is the data collected after 9 months of the case, while (d) is the data collected after one year.

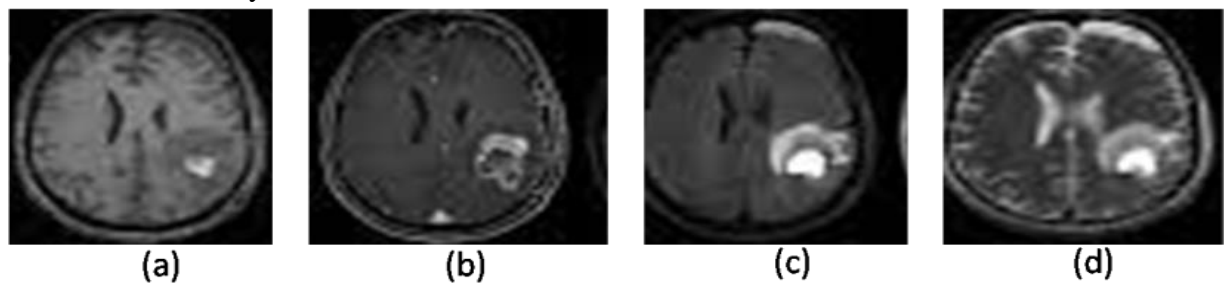


Figure 1: Data sample of GBM at different stages over one year period

Figure 1 report sample GBM collected from one patient over one year period ranging from one month, 3 month, 9 month and one year case of GBM. Overall the sample size of data collected for GBM is 300, considering 13 patients. Figure 2 reported data collected from another patient with mixed glioma at different stages.

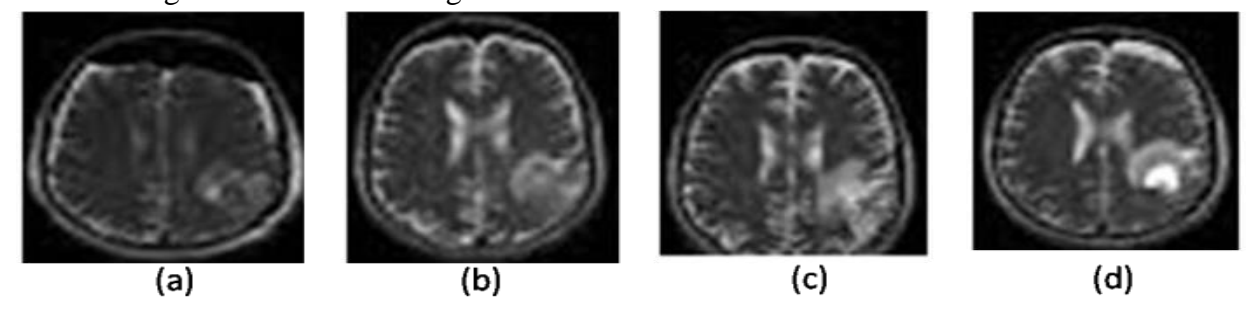


Figure 2: Data sample of mixed gliomas at different states over one year period

Figure 2 reported results of data collection from a patient. (a) was collected when the patient has one month case; (b) was collected at 5 months; (c) was collected at 7 months while (d) was collected at one year. The total subjects which provided data of this class are 7 and the overall sample size is 89. Figure 3 presents the sample of data collection from patients with meningiomas over one year period. (a) was collected at 4 month, (b) was collected at 7 months and (c) was collected at one year. The sample size of data collected is 260, when the number of subject is 14. Figure 4 also reported samples of data collected from Ependymomas infected patient.

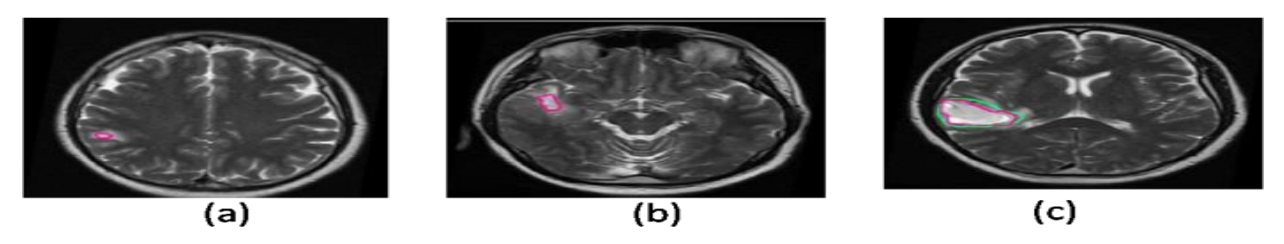


Figure 3: Sample from patient with Meningiomas

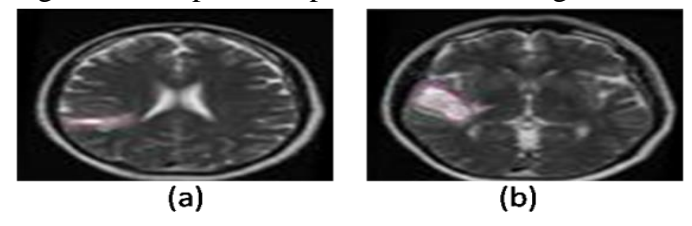


Figure 4: Sample from patient with Ependymomas

Figure 4 presents the sample of data collected from an Ependymomas infected patient. The data was collected from patient with one year confirmed case. The Figure 4 (a) was collected at 3 month while figure (b) was collected at 7month. The total sample size of data collected is 45 from 5 patients. The total sample size of primary data collected is 694, while the number of subjects is 39. A secondary data source was also collected from the Roboflow repository considering 10000 samples of glioma across the four different classes, and 145 Nigerian participants. Overall, the total sample size of data collected is 10, 694, while the number of subjects is 184.

2.2 Model of the CNN

CNN is a state-of-the-art deep learning model which has been applied to solve image classification problem. CNN has four main components which are the input layer, the convolutional layer, the fully connected layer and the output layer as shown in Figure 5.

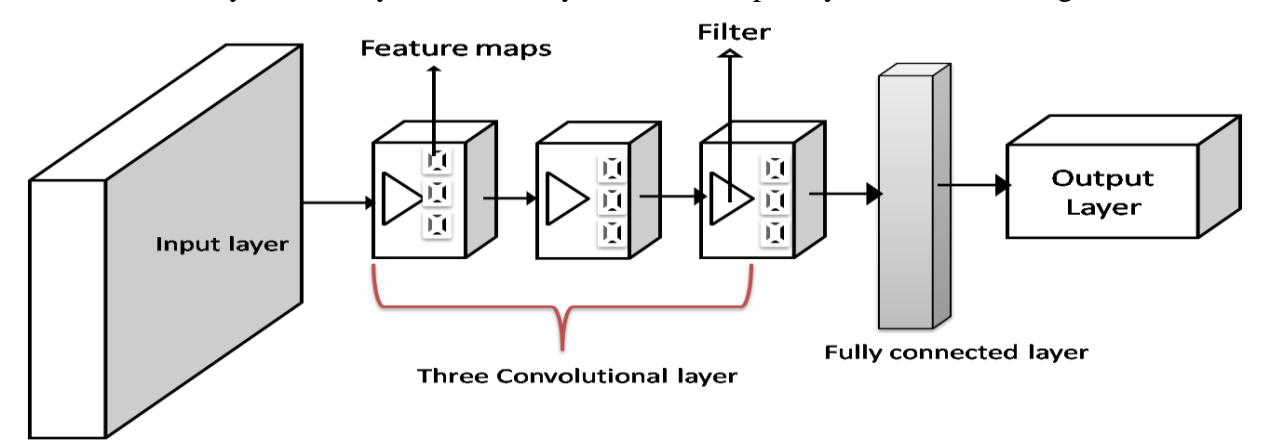


Figure 5: Basic CNN Block diagram

The input facilitates dimensioning of the images to the network, the convolutional layer is responsible for rich feature extraction process using filters, the features are then trained in the fully connected layer and produce result in the output layer. The most crucial part of the CNN is the convolutional layer, and employed several filters to scan the feature maps, and then pooling

layer to extract information from the image dataset. The output of these layers is determined through the model in Equation 1 (Asiri et al., 2023).

$$FM_h^a = \Delta(K_h^a - I_L + Y^i) \tag{1}$$

Where FM_b^a the feature is maps resulting from the data, Δ is the activation function, I_L is the input weight, and Y^i is the filter channel. The sizes of the features extracted are presented in Equation 2 (Asiri et al., 2023);

$$Size = \frac{input-filter}{stride} + 1 \tag{2}$$

The Equation 1 is the features maps extracted from the input images, while the Equation 2 defines the size of the features extracted by the CNN filter. The pooling layer is a component of the CNN which ensures the features maps identified from the convolutional filter scan are gathered for training and model based on the design. Pooling techniques used for this work is the maximum pooling approach, while the filter size is 3 by 3. The size pooling layer size is calculated as shown in Equation 3, while the size of the feature pooled is defined by Equation 4 (Ji et al., 2020).

$$P_{i,j} = \max_{p,s \in R} \tag{3}$$

Pooling layer output size =
$$\frac{convolutional\ output-pooling\ size}{strides}$$
 (4)

2.2.1 To model ResNet50 model

The ResNet50 is a 50 layered residual network made of input layers, several convolutional layers, connected in batches and then the fully connected layer as shown in the architecture of Figure 6. The ResNet50 is a type of CNN already trained with ImageNet dataset for object detection and recognition task (He et al., 2016; Muñoz-Saavedra et al., 2023). The ResNet-50 block constitutes several layers such as convolutional layer, batch normalization, and rectified linear unit and identity short connections. This component allows the network to learn residual mapping during the training. The convolutional block allows dimensionality adjustment and downsampling of samples. Overall, the layers are 50 with the final layer constituting the average pooling layer, flattened layer and fully connected layer. Upon training the model, it can be applied for classification tasks.

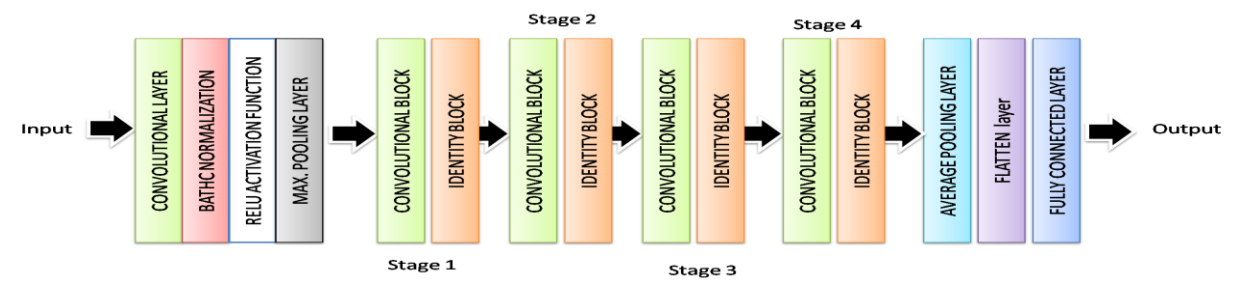


Figure 6: The ResNet-50 block diagram

The Figure 6 of the ResNet-50 is made of the convolutional block which performs feature identification from the input layer. The batch normalization stabilizes training process and acceleration of convergence. The activation function introduces nonlinearity to learn complex patterns in the data. Max and average pooling function reduced spatial weight dimension and

computational complexity. The convolutional block combines the batch normalization, RELU with a short connection to learn residual maps. The identity block ensures input dimension of the data is preserved while learning residual maps. The features are flattened into 2D vectors before training in the fully connected layer section.

2.2.2 U-Net

The encoder reduces spatial dimensions while preserving context by extracting hierarchical features using convolution and max pooling. Processing deep feature representations, the bottleneck serves as a transition. In order to restore spatial resolution, the decoder uses transposed convolutions to upsample the compressed features. To ensure accurate localization, Skip connections send fine-grained information straight from the encoder to the decoder. In order to create the final segmentation mask, the output layer employs a 1×1 convolution with activation (SoftMax or sigmoid), which makes U-Net efficient for pixel-wise classification tasks.

2.2.3 Proposed CNN + ResNet50+U-Net Model (CNN-ResNet)

The proposed CNN+ResNet were developed with the combination of the CNN, ResNet-50 and U-NET. The CNN was fine tuned with the connection of the convolutional layers to the ResNet combined with U-Net. The fully connected layer in the CNN was replaced with the ResNet+ U-Net as shown in the Figure 7, while in Figure 8; the MRI data was imported to the model for training to generate the classifier.

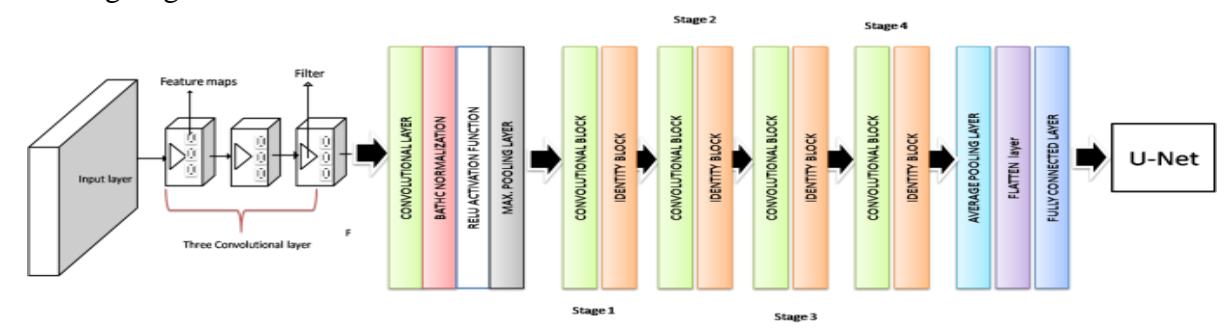


Figure 7: Architecture of the CNN+ResNet+ U-Net

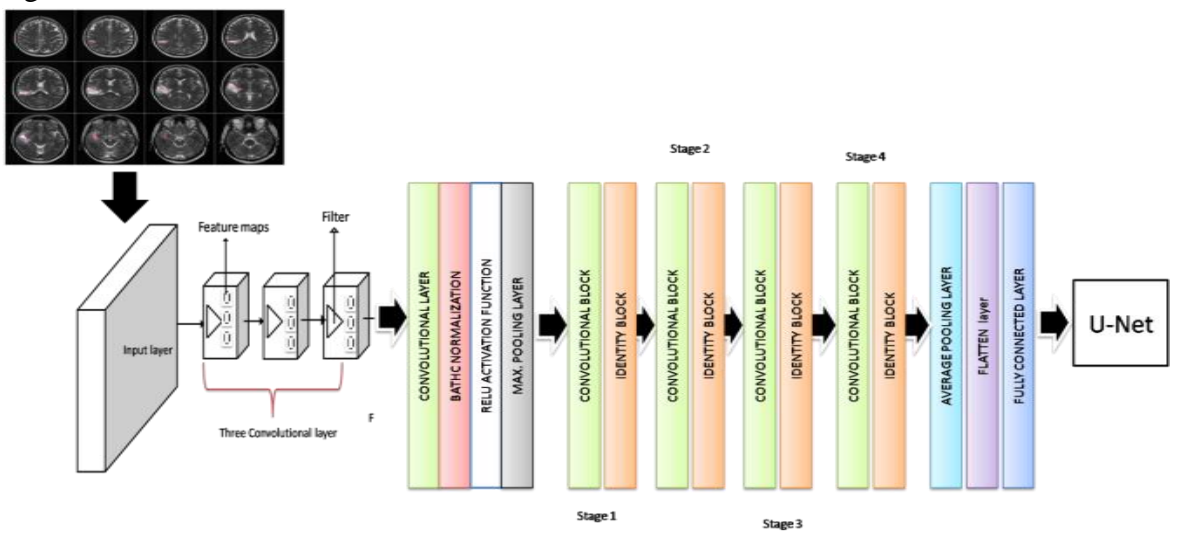


Figure 8: Architecture of the CNN+ResNet+U-Net with the loaded MRI data of glioma

Figure 7 present the CNN+ResNet +U-net architecture, while in the Figure 8, the MRI data collected was imported to the new deep learning model for training and generation of the classifier.

2.3 Training of the model

The CNN + ResNet50 + U-Net model was trained by combining the advantages of U-Net for pixel-level feature localization, ResNet50 for deeper learning capabilities with residual connections, and convolutional neural networks (CNNs) for feature extraction. To improve robustness and avoid overfitting, data augmentation techniques were applied to the dataset prior to preprocessing. With a learning rate of 0.001, the model was optimized during training using the Adam optimizer, with categorical cross-entropy serving as the loss function. 50 epochs of training were conducted, and the dataset was divided into training (80%) and validation (20%) sets. The training involved also several experiments on the deep leaning models such as ResNet-50, ResNet+CNN and ResNet+CNN+Unet, were all separately trained to validate out model further. When it came to differentiating between glioblastoma multiforme, oligodendroglioma, ependymomas, and mixed glioma, the model demonstrated efficacy by achieving high training and validation standards, which are all reported in chapter five. The tool used for the process is python programming language.

2.4 To develop the model of the brain tumor classification system

To develop the deep learning model for brain tumor classification, the deep learning algorithm proposed was trained and the performance evaluated. Upon meeting stopping criteria, the model for the detection of brain tumor was generated. Figure 9 present the system flowchart, which showed that when input data was loaded to the model, it is processed and then feed to the trained classifier which then began the classification process. Upon complete classification using the ResNet, the object classified is then identified and labelled by the RPN.

2.5 System Implementation

The software system for glioma classification was implemented using Python, utilizing its powerful libraries such as TensorFlow, Keras, NumPy, and Matplotlib. The system integrates a CNN + ResNet50 + U-Net architecture, optimized to classify glioblastoma multiforme, Meningioma, ependymomas, and mixed glioma. The model leverages CNN layers for feature extraction, ResNet50 for deep residual learning, and U-Net for precise segmentation and spatial feature localization. Python's seamless integration capabilities allowed efficient pre-processing of the dataset, which included data normalization, augmentation, and splitting into training and validation sets. A user-friendly interface was created to enable easy input of MRI scans, while the backend handles image pre-processing and prediction tasks.

The implementation process focused on ensuring scalability and accuracy, with the software achieving high-performance metrics during testing. The system was trained using Python's TensorFlow library, utilizing an Adam optimizer and categorical cross-entropy loss function to minimize errors. The training process incorporated GPU acceleration for faster computations, ensuring quick iteration through the epochs. Results from the classification are displayed in an interactive dashboard, providing users with the predicted glioma type and confidence scores for

each class. Python's visualization libraries, such as Matplotlib and Seaborn, were used to present training progress (accuracy and loss curves) and to plot confusion matrices for performance evaluation, ensuring the system's transparency and reliability.

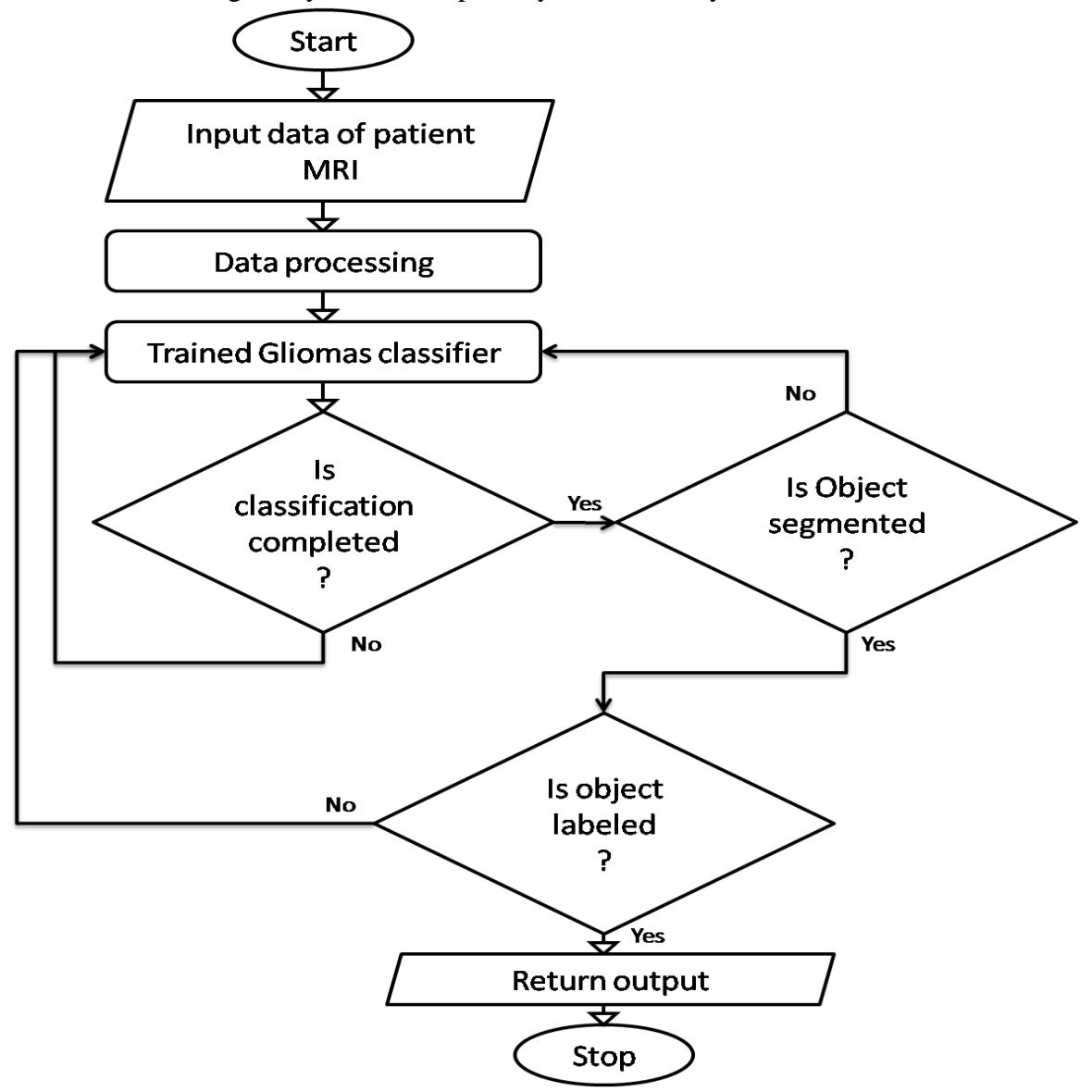


Figure 9: Flow chart of the glioma classification model

3. RESULTS AND DISCUSSIONS

3.1 Result of the transfer learning model training

This section presents the results of the transfer learning model training, beginning with the evaluation of the individual performance of the ResNet50 model. This is followed by an analysis of the combined ResNet + CNN model, and then the ResNet + CNN + U-Net hybrid model, which explores the impact of integrating advanced architectures. Additionally, the section

provides a comparative analysis of these trained models to understand their relative strengths. Finally, a broader comparison with existing models in the field is conducted to highlight the improvements and effectiveness of the proposed methods.

3.2 Result of the ResNet50

The result of the experimental training of the ResNet-50 was presented in this section considering accuracy and loss function during training and validation. The accuracy measures the success of classification at different epoch while the loss measures the error which occurred during the training process, when comparing the true and predicted values in the data. Figure 10 presents the training results.

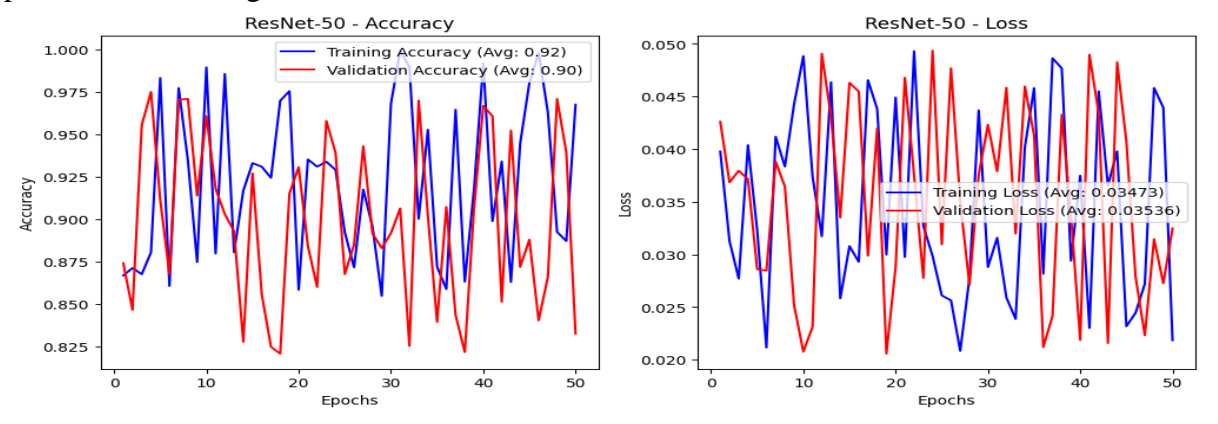


Figure 10: Result of the model training and loss performance

The Figure 10 presents the training and loss performance of the ResNet when trained with data of glioma. The results recorded accuracy of 0.92 for training and validation accuracy of 0.90, while the training loss reported 0.03473 and 0.03536 for validation. Overall, these results revealed the effectiveness of ResNet in correctly classifying glioma, with high accuracy rate of 90%. The Figure 11 presents the confusion matrix results.

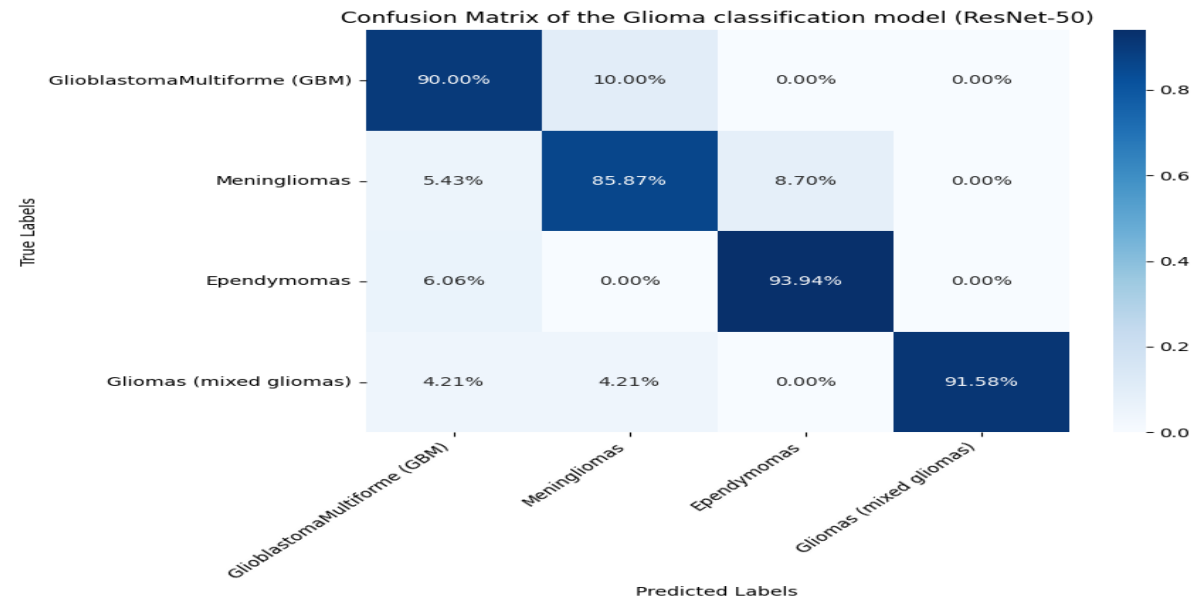


Figure 11: Confusion matrix of the ResNet model

The Figure 11 presents the confusion matrix of the ResNet model during testing. From the results, the GBM reported 90% True Positive Rate (TPR), 10% False Positive Rate (FPR) was reported for Meningioma, while 0% for the other two classes respectively. This suggested that the ResNet model was able to correctly classify GBM with 90% success rate, while 10% of the data was mistaken for another class which is Meningioma. In the next diagonal matrix, it was observed that Meningioma reported 85.87%, Ependymomas reported 93.94% TPR while mixed glioma reported 91.58% TPR. Overall, the results have demonstrated the ability of the trained ResNet to correctly classify glioma types to help in the diagnosis of patients with brain disease.

3.3 Result of the CNN Model Training

This section reported the results of the CNN model after training and validation. The Figure 12 reported the results obtained.

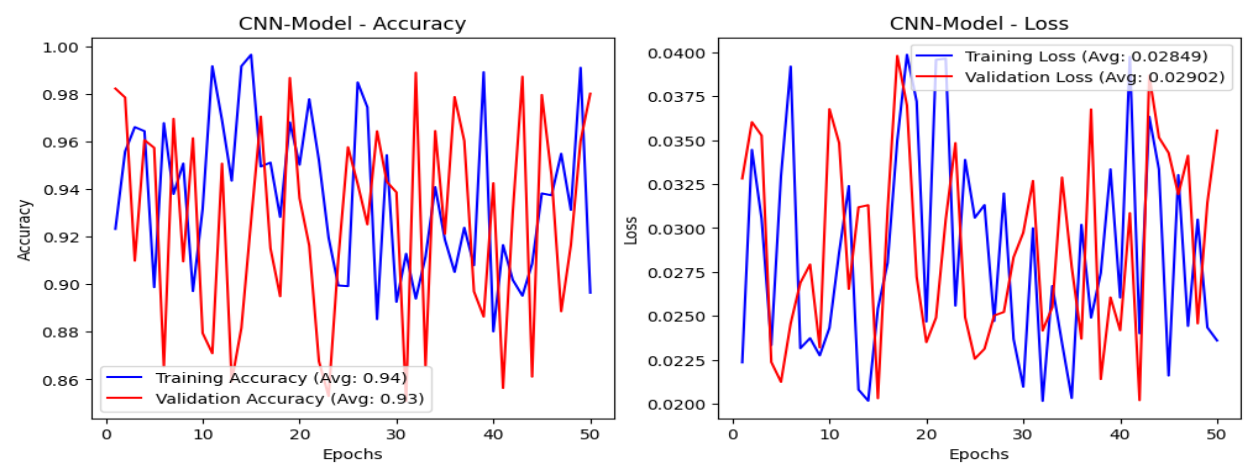


Figure 12: Result of the CNN Model

Figure 12 presents the results of the CNN. From the result, it was observed that the accuracy reported 0.94 for training and 0.92 for validation. The loss function reported training loss value of 0.02920, and validation loss of 0.02953. These results implied that the model of CNN was able to record high accuracy in classifying different classes of glioma. The confusion matrix of the model performance was reported in Figure 13.

From the Figure 13, it was observed that GBM recorded True Positive rate (TPR) of 92%, and False Positive Rate (FPR) of 8% with 6% of the FPR classified for Mininglioma while 2% classified as mixed glioma. The Mininglioma was correctly classified as 85%, with 10% FPR for ependymomas and 5% FPR for GBM. Ependymomas reported 93.94% TPR and then a 6.06% FPR of GBM. Finally the mixed glioma reported 91% TPR, 4% FPR for GBM, 5% for Mininglioma.

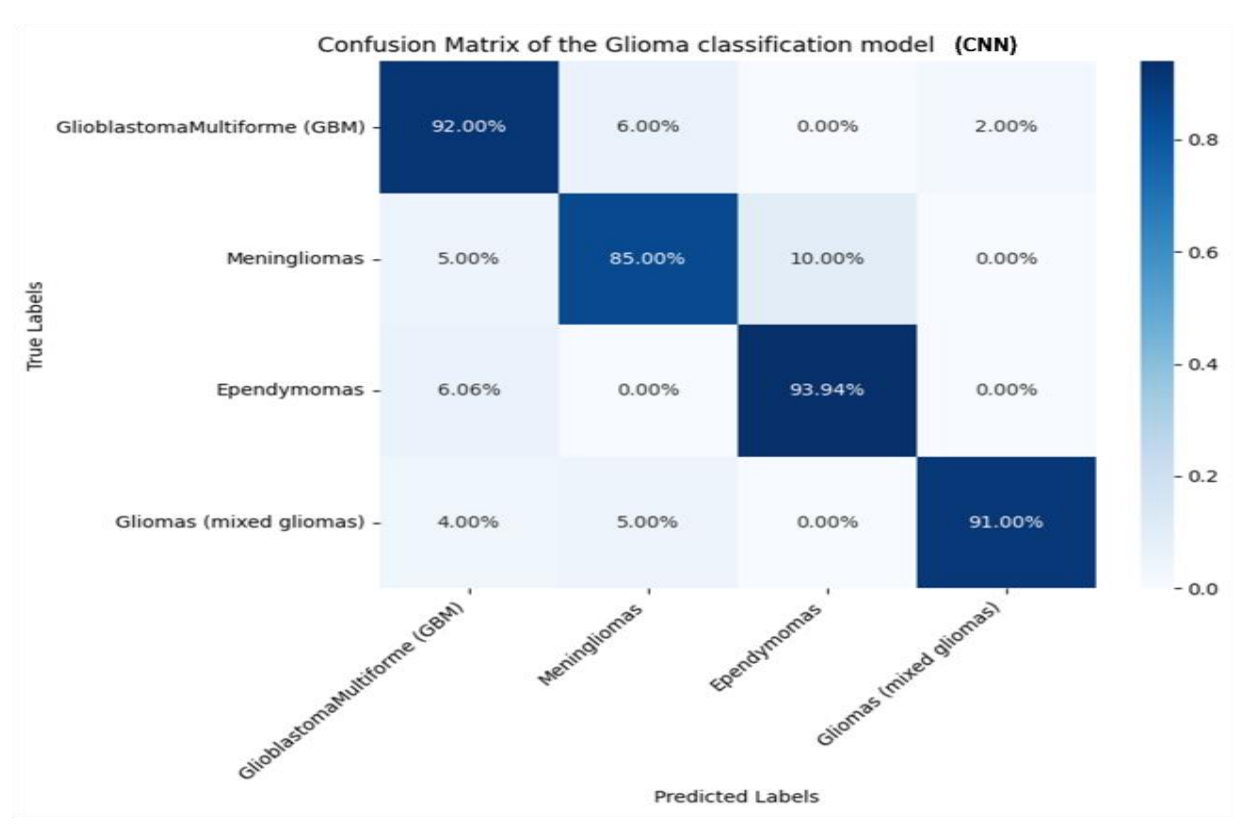


Figure 13: Confusion matrix of the CNN+ ResNet Model

3.4 Result of the ResNet + CNN+ U-Net

This section presents the training results of the ResNet + CNN+UNET. The results recorded the training and validation results of the transfer learning model. Figure 14 present the results of accuracy and loss value for the proposed ResNet which constitutes ResNet + CNN+U-NET. The Figure 15 presents the accuracy which reported 0.95 for training and 0.94 for validation. For the loss, the training reported 0.02875 and validation loss 0.02815; while the confusion matrix was reported in Figure 15.

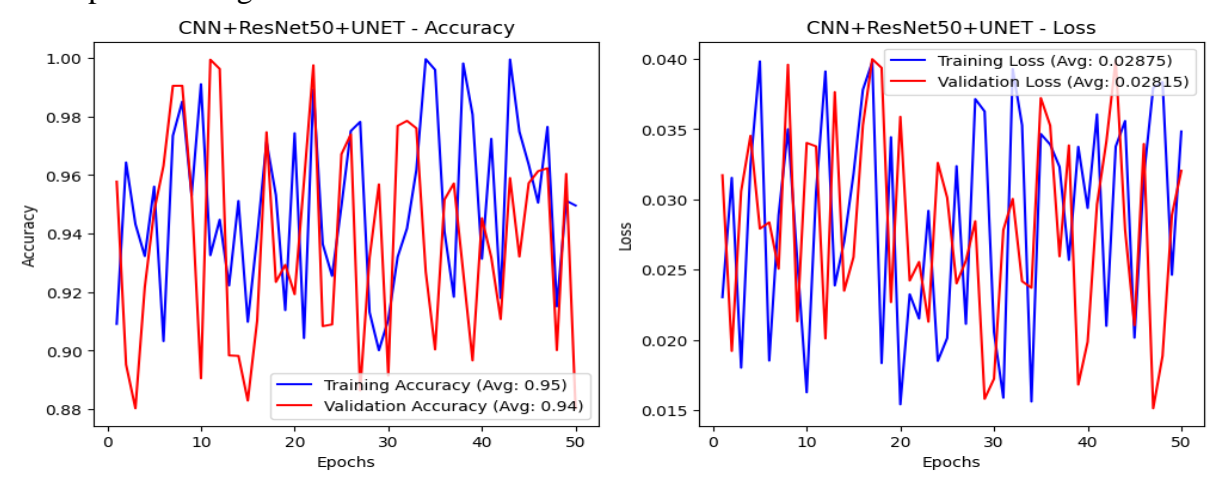


Figure 14: Result of the accuracy and loss for the ResNet + CNN+UNET.

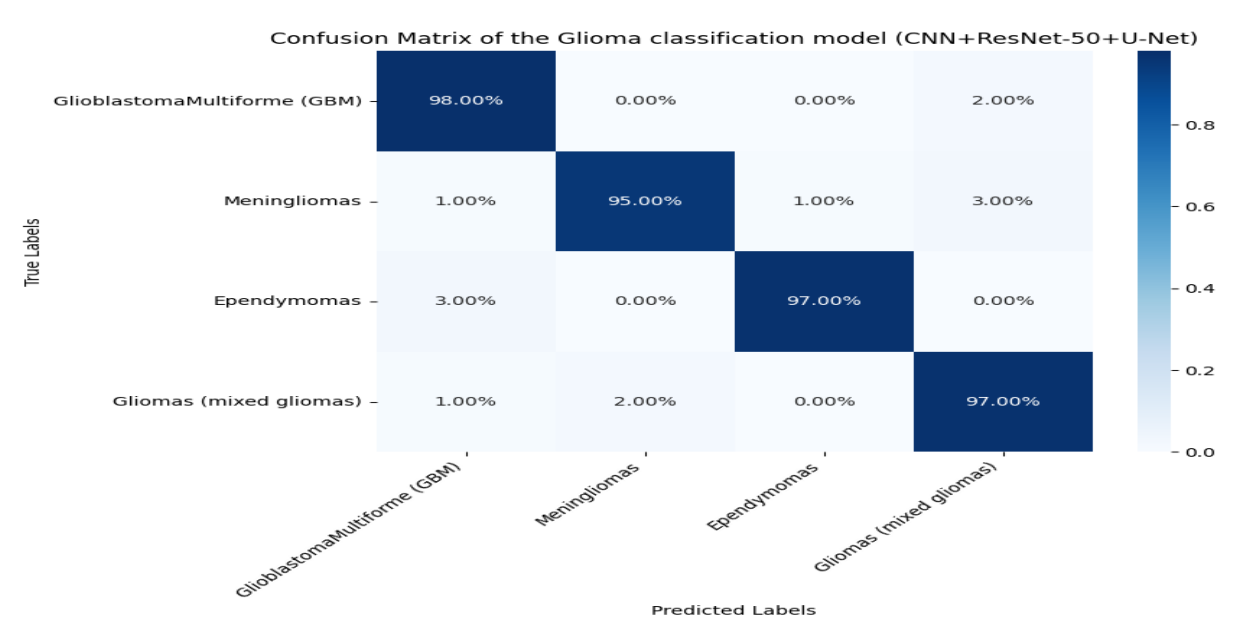


Figure 15: Confusion matrix of the ResNet + CNN+UNET

Figure 15 revealed the ResNet + CNN+UNET was able to correctly classify the four classes of the glioma. The results for GDM reported 98% and 2% for mixed glioma. Mininglioma reported 95% TPR, Ependymomas reported 97% TPR and mixed glioma which reported 97%. Overall, these results have demonstrated the effectiveness of the new model proposed and trained for classification of several types of glioma.

3.5 Comparative Analysis of trained models

This section presents a comparative analysis of the three models trained and evaluated in this work for the classification of glioma. The Table 1 presents the summarized results.

Table 1: Comparative analysis

Model	Accuracy	Loss
ResNet	0.90	0.03473
CNN	0.92	0.02953
ResNet+CNN+ UNET	0.95	0.02815

The results in Table 1 compared the performance of the experimental deep learning model trained with data of BTI classifying different glioma. From the results it was observed that overall while the three models recorded high accuracy and tolerable loss function values; the ResNet+CNN+UNET reported an accuracy of 95% and loss of 0.02815 as the best when compared to other models. Based on this, the model was applied for system integration.

3.6 Result of Practical Validation to validate the work

In this section of system integration, the results of the software developed after testing with real world glioma data was reported. The Figure 16 reported the result of the glioma test data, while the output results after classification and object detection was reported in Figure 17. To ensure more consistency in the results, we applied other glioma MRI test samples to validate the software. The results are reported in the Figure 18 and 19 respectively. In the Figure 20, the test

data of meninglioma was presented, to validate the ability of the model for multiple classes of glioma.

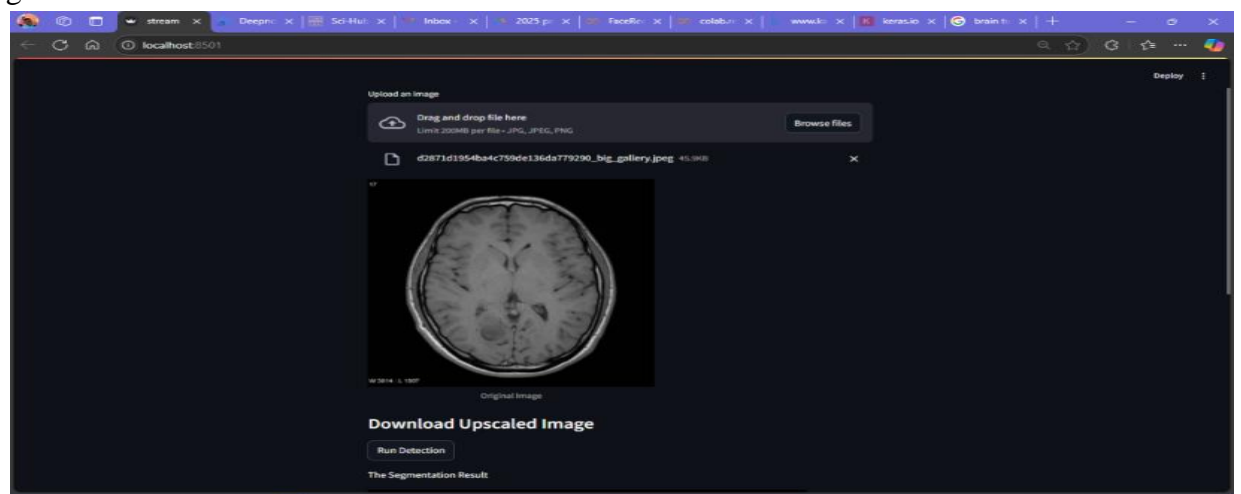


Figure 16: Result of the Test Mixed Glioma MRI Data

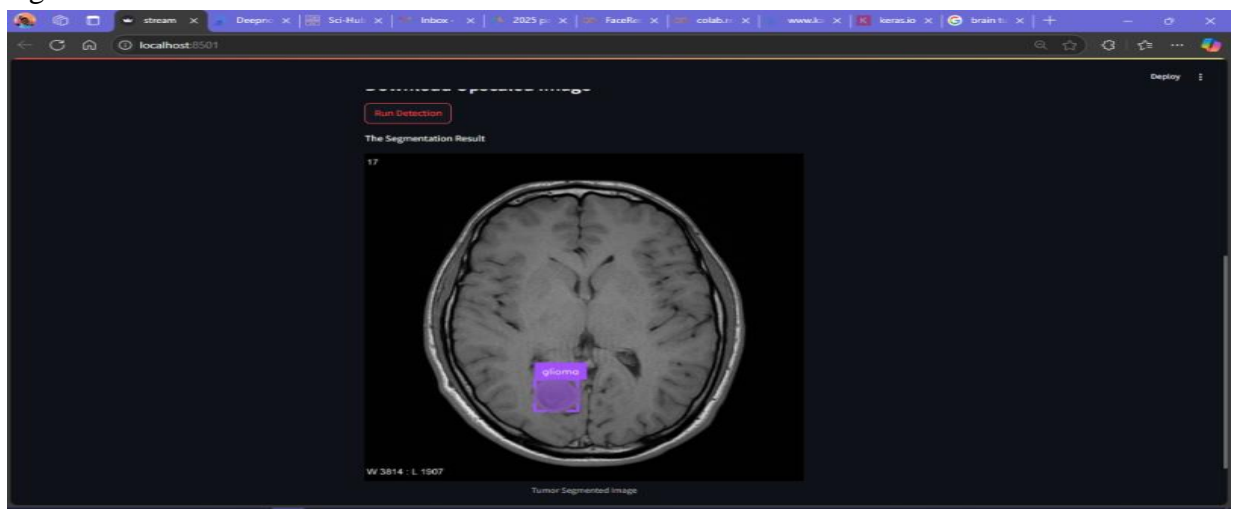


Figure 17: The results of the glioma classification and detection (case 1)

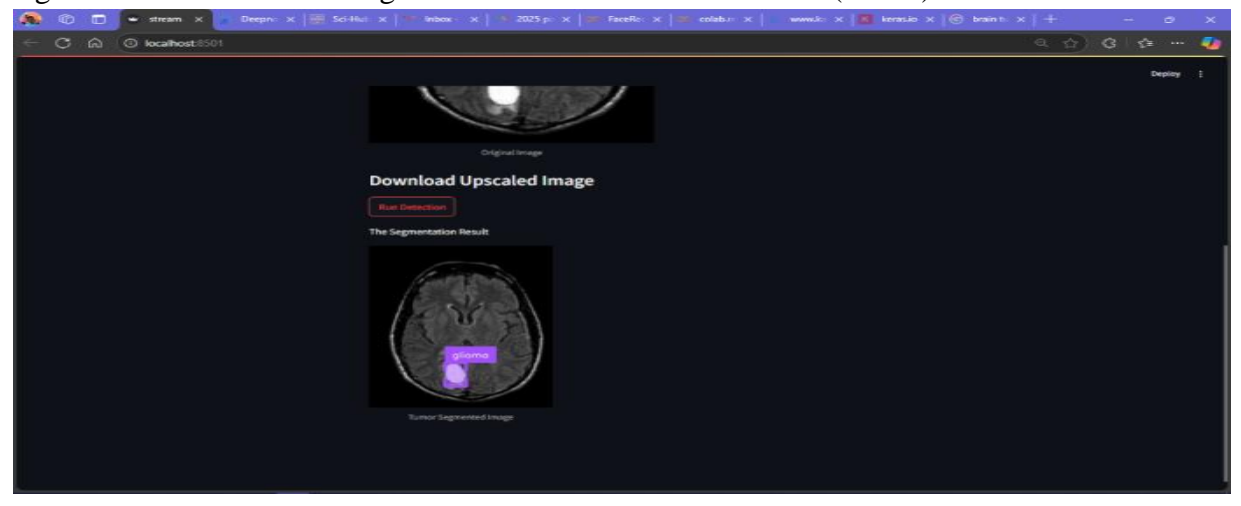


Figure 18: The experimental result of glioma test (case 2)

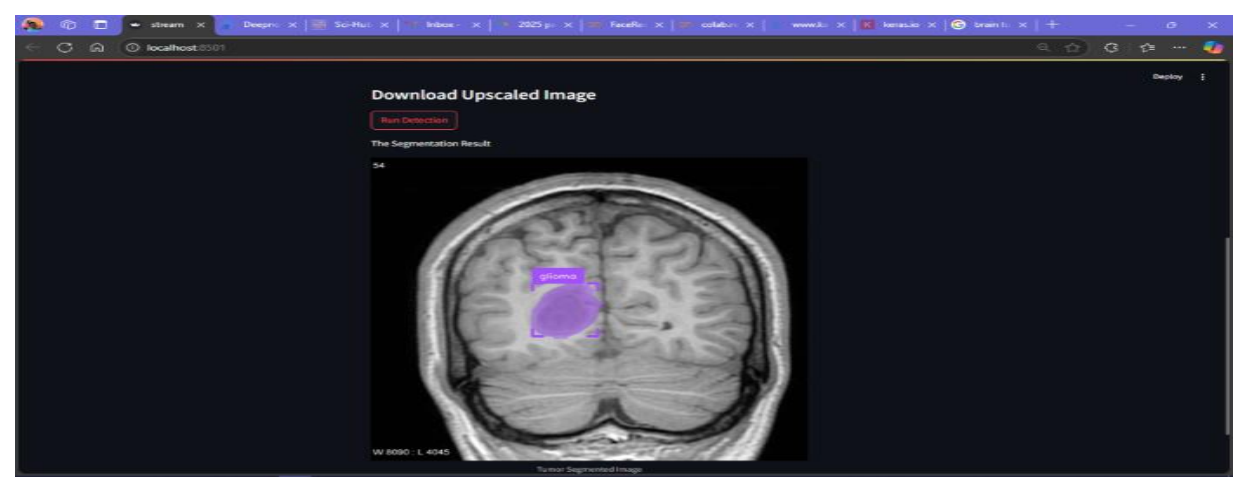


Figure 19: Experimental result of glioma test (case 3)

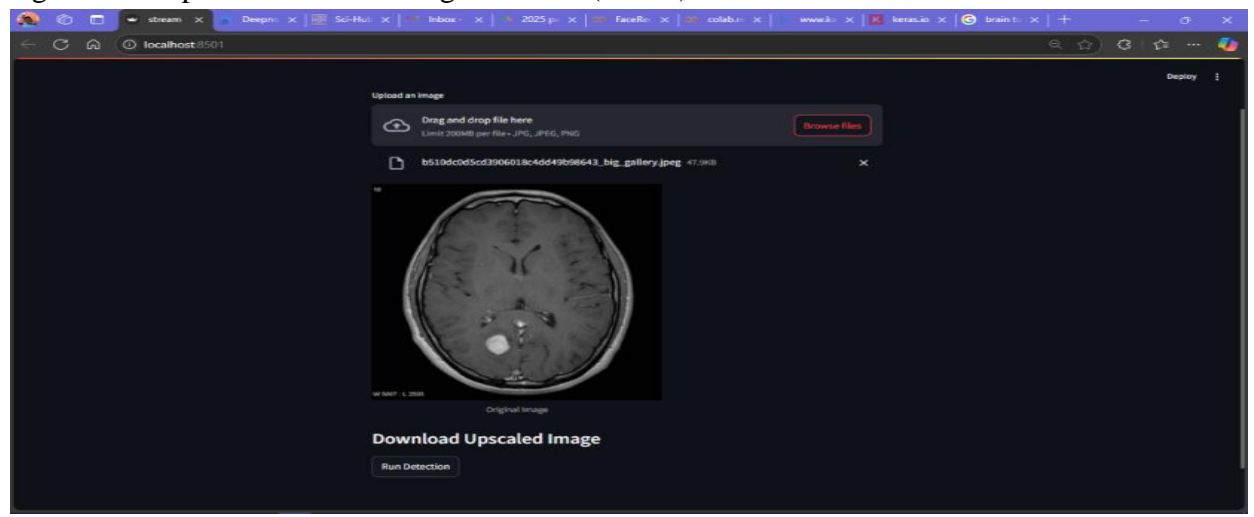


Figure 20: Test data of meninglioma

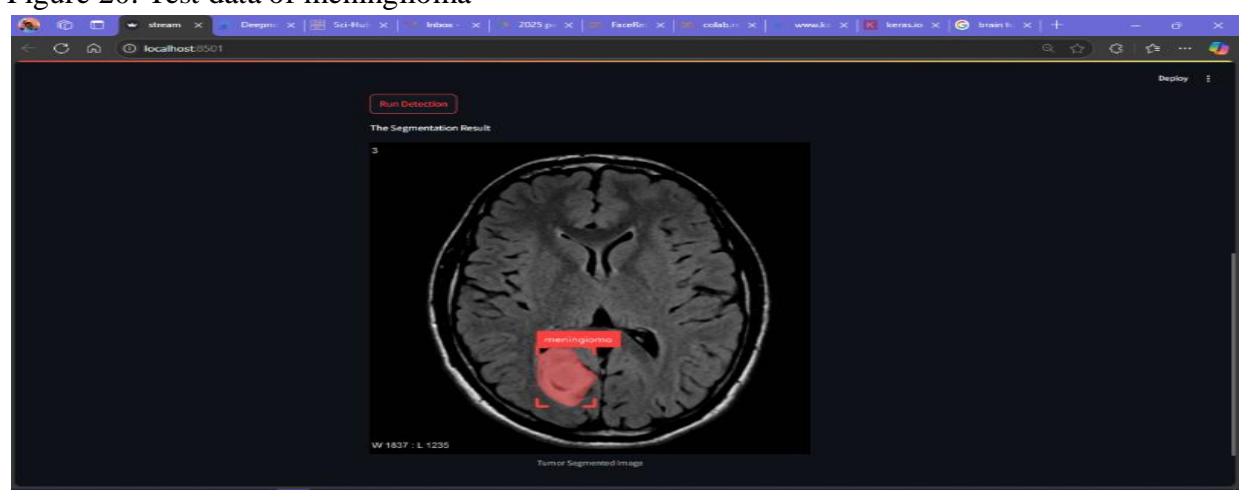


Figure 21: Result of the mininglioma classification

Figure 20 presented the test data of the meninglioma. The Figure 21 reported the result of the meninglioma which was classified by the CNN+ResNet+Unet. This was achieved through

feature extraction by the CNN, then the ResNet classified the image as meniglioma infected and the UNET identify the segment of the image infected and then segment with label.

4. CONCLUSION

This study developed a deep learning-based system for the classification and segmentation of glioma using MRI data. The methodology adopted in this study combined CNNs for feature extraction, ResNet50 for deep residual learning and U-Net for precise spatial segmentation. MRI data were gathered from two sources: primary data from Memfy's Hospital and secondary data from the Roboflow repository, totalling 10,694 samples covering four glioma types such as Glioblastoma Multiforme (GBM), Meningioma, Ependymomas, and Mixed Glioma. This diverse dataset enabled thorough model training and robust evaluation. The experimental results from the study implementation showed that the hybrid CNN+ResNet50+U-Net model outperformed individual models, achieving a training accuracy of 95% and a validation accuracy of 94%, along with low loss values. Analysis of the confusion matrix confirmed that the model could reliably classify and segment all glioma types, surpassing the performance of standalone CNN or ResNet50 models. Furthermore, practical validation using real-world MRI test cases demonstrated the model's ability to accurately localize, classify, and segment tumors.

In summary, this study highlights that integrating CNN, ResNet50, and U-Net provides a highly effective framework for automated glioma detection. The hybrid approach improves classification accuracy, supports multi-class tumor identification, and delivers precise segmentation, making it well-suited for clinical applications. This system offers a dependable tool to assist radiologists in brain tumor diagnosis and lays the groundwork for future AI-driven medical imaging research.

5. REFERENCES

- Adefisayo, A., Peters, K., et al. (2019). Neurooncology research in Nigeria: Great untapped potential. *World Neurosurgery*, 124, 381–385.
- Alqudah, A., Alqurann, H., Qasmieh, I., Alqudah, A., & Al-Sharu, W. (2019). Brain tumor classification using deep learning technique A comparison between cropped, uncropped, and segmented lesion images with different sizes. *International Journal of Advanced Trends in Computer Science and Engineering*, 8(6), 3684–3691. https://doi.org/10.30534/ijatcse/2019/155862019
- Ankita, P. (2020). Brain tumor detection using deep learning. Birla Vishvakarma Mahavidyalaya (Engineering College).
- Asiri, A. A., Shaf, A., Ali, T., Aamir, M., Irfan, M., Alqahtani, S., ... &Alqhtani, S. M. (2023). Brain tumor detection and classification using fine-tuned CNN with ResNet50 and U-Net model: A study on TCGA-LGG and TCIA dataset for MRI applications. *Life*, *13*(7), 1449. https://doi.org/10.3390/life13071449
- Deborah, U. E., Onyianta, J. C., Erhunmwunsee, D. O., & Ihudiebube, C. N. (2022). Determining the predictive performance of hybrid classification algorithms on COVID-19 patient death

- rate in Nigeria. International Journal of Mechatronics, Electrical and Computer Technology (IJMEC), 12(44), 5191–5194.
- He, K., Zhang, X., Ren, S., & Sun, J. (2016). Deep residual learning for image recognition. In *Proceedings of the IEEE Conference on Computer Vision and Pattern Recognition* (pp. 770–778).
- Hussain, A. (2021). Brain tumor detection in magnetic resonance imaging using deep learning approach. Qatar University: Research Square. https://doi.org/10.21203/rs.3.rs-2281460/v1
- Jie, H. J., & Wanda, P. Run. (2020). A dynamic pooling layer for convolution neural network. *International Journal of Computational Intelligence Systems*, 13, 66–76.
- Louis, D., Perry, A., Reifenberger, G., von Deimling, A., Figarella-Branger, D., Cavenee, W. K., ... & Ellison, D. W. (2016). The 2016 World Health Organization classification of tumors of the central nervous system: A summary. *Acta Neuropathologica*, *131*, 803–820.
- Mahmud, M., Mamun, M., & Abdelgawad, A. (2023). A deep analysis of brain tumor detection from MR images using deep learning networks. *Algorithms*, 16, 176. https://doi.org/10.3390/a16040176
- Muhammad, I., Sharif, M., Khan, M. A., Alhussein, M., Aurangzeb, K., & Raza, M. (2022). A decision support system for multimodal brain tumor classification using deep learning. *Complex & Intelligent Systems*, 8, 3007–3020. https://doi.org/10.1007/s40747-021-00321-0
- Muñoz-Saavedra, L., Escobar-Linero, E., Civit-Masot, J., Luna-Perejón, F., Civit, A., & Domínguez-Morales, M. (2023). A robust ensemble of convolutional neural networks for the detection of monkeypox disease from skin images. *Sensors*, *23*(16), 7134. https://doi.org/10.3390/s23167134
- Perkins, A., & Liu, G. (2016). Primary brain tumors in adults: Diagnosis and treatment. *American Family Physician*, 93, 211–217.
- Qureshi, S. A., Raza, S. E. A., Hussain, L., Malibari, A. A., Nour, M. K., Rehman, A. U., ... & Hilal, A. M. (2022). Intelligent ultra-light deep learning model for multi-class brain tumor detection. *Applied Sciences*, 12, 3715. https://doi.org/10.3390/app12083715
- Saman, S., & Narayanan, S. (2018). Survey on brain tumor segmentation and feature extraction of MR images. *International Journal of Multimedia Information Retrieval*. https://doi.org/10.1007/s13735-018-0162-2
- Sharif, M., Amin, J., Raza, M., Yasmin, M., & Satapathy, S. C. (2020). An integrated design of particle swarm optimization (PSO) with fusion of features for detection of brain tumor. *Pattern Recognition Letters*, 129, 150–157.